Carbohydrate Polymers 201 (2018) 634–642

Contents lists available at ScienceDirect

Carbohydrate Polymers

journal homepage: www.elsevier.com/locate/carbpol

Fucosylated chondroitin sulfate oligosaccharides from *Isostichopus badionotus* regulates lipid disorder in C57BL/6 mice fed a high-fat diet

Shan Li[a], Junhui Li[a], Guizhu Mao[a], Yaqin Hu[a], Xingqian Ye[a], Ding Tian[a], Robert J. Linhardt[b], Shiguo Chen[a,*]

[a] Zhejiang Key Laboratory for Agro-Food Processing, Department of Food Science and Nutrition, Fuli Institute of Food Science, Zhejiang University, Hangzhou, 310058, China

[b] Center for Biotechnology and Interdisciplinary Studies, Rensselaer Polytechnic Institute, Troy, New York 12180, USA

ARTICLE INFO

Keywords:
Sea cucumber
Fucosylated chondroitin sulfate
oligosaccharide
Lipid disorder
High-fat diet
Transcriptome analysis

ABSTRACT

Fucosylated chondroitin sulfate (fCS) and its depolymerized derivative (DfCS), prepared from sea cucumbers, are well-known for their anticoagulant activity. However, their other functional activities are poorly understood. Recently, we obtained fCS oligosaccharides from *Isostichopus Badionotus* by a modified controllable Fenton-system, named as DfCS-*Ib*. The functional activities of these oligosaccharides are still unclear. The present study investigated anti-hyperlipidemic activity of DfCS-*Ib* using a high-fat diet (HFD)–fed mice model. The results indicated that DfCS-*Ib* reduced obesity, hyperlipidemia, and inflammation caused by HFD. Meanwhile, DfCS-*Ib* increased the mRNA expression of PPARγ and decreased the mRNA expression of leptin, aP2, and F4/80 in fat tissue. Transcriptome analysis indicated that DfCS-*Ib* normalized the expressions of genes regulating lipid metabolism. Our results suggested that DfCS-*Ib* can alleviated lipid disorder by reducing lipid synthesis and promoting lipid lipidolysis. DfCS-*Ib* can act as a functional agent to regulate lipid disorder.

1. Introduction

Dyslipidemia has been a serious risk for human health by causing serious consequences. Over nutrition, such as Western diet, is a major contributor to dyslipidemia (Cordain et al., 2005). In addition, excessive energy intake often brings other complications such as obesity, inflammation, and nonalcoholic fatty liver disease (NAFLD). Diets typically high in animal fats, high in simple sugars and low in plant-based fibers, are referred to as a high-fat diet (HFD). HFD is often used in most studies to mimic diseases related to dyslipidemia (Noeman, Hamooda, & Baalash, 2011; Wang et al., 2017a). Dyslipidemia is characterized by elevated concentrations of serum triglycerides (TG), total cholesterol (TC), and low-density lipoprotein cholesterol (LDL-C) (Kotani, Serban, Penson, Lippi, & Banach, 2016). Adipose tissue and liver are the most important energy tissues and organs for lipid metabolism. Excessive energy intake will disturb the normal function of adipose tissue and liver (Kakimoto & Kowaltowski, 2016; Ouchi, Parker, Lugus, & Walsh, 2011) by influencing expression of genes related to energy metabolism. Thus, it is very important to maintain the normal function of adipose tissue and liver.

Polysaccharides have powerful effects on regulating dyslipidemia (Cao et al., 2016; Pan et al., 2016). Extensive evidence indicates that polysaccharides can regulate lipid metabolism through multi-functional roles. Polysaccharide from *Angelica sinensis* can reduce lipid accumulation and inflammatory response caused by HFD (Wang et al., 2015). Chitosan reduces energy intake by promoting fecal TC, TG, and total bile acid (TBA) excretion in *vivo* (Zhang, Zhang, Mamadouba, & Xia, 2012). This may result from the lipid-binding ability of chitosan, as a type of a cationic polysaccharide (Wydro, Krajewska, & HąC-Wydro, 2007). Fucoidan can reverse the disorders related to protein expression caused by over nutrition, such as normalizing PI3K/PKB/GSK-3β signaling in liver tissue (Wang et al., 2016) and GLUT4/PI3K/PKB in adipose tissue (Huang et al., 2016). Glycosaminoglycans from crickets can affect liver gene expression profiling in rats on a HFD and exert antilipidemic effects (Ahn, Hwang, Kim, & Park, 2016). Most studies on the effects of glycans on lipid disorders have been focused on polysaccharides. However, to the best of our knowledge, there is a very limited research involving the impact of glycans on lipid disorders at the oligosaccharides level.

Fucosylated chondroitin sulfate (fCS) from sea cucumbers is a kind

Abbreviations: HFD, high-fat diet; fCS-*Ib*, chondroitin sulfate from *Isostichopus badionotus*; DfCS-*Ib*, degraded chondroitin sulfate from *Isostichopus badionotus*; TC, total cholesterol; TG, triglyceride; HDL-C, high density lipoprotein cholesterol; LDL-C, low density lipoprotein cholesterol

* Corresponding author at: College of Biosystem Engineering and Food Science, Zhejiang University, Hangzhou, 310058, China.
E-mail address: chenshiguo210@163.com (S. Chen).

https://doi.org/10.1016/j.carbpol.2018.08.020
Received 23 April 2018; Received in revised form 5 August 2018; Accepted 5 August 2018
Available online 06 August 2018
0144-8617/

of glycosaminoglycan composed of alternating β-D-glucuronic acid and *N*-acetyl-β-D-galactosamine units with α-L-fucose branches. The most attractive property of fCS is their specific repeating oligosaccharide units and their unique sulfation patterns. This family of glycosaminoglycans has been extensively studied for its anticoagulant and antithrombotic activities for its sulfation (Chen et al., 2011). In addition, fCS also demonstrates health benefits in energy metabolism by normalizing the function of adipose tissues and liver (Hu et al., 2013) and inhibiting lipid disorders caused by over nutrition (Wu et al., 2016). Recently, depolymerized fCS (DfCS) from sea cucumbers has attracted increasing attention due to its reduced adverse effects on anticoagulation, compared to polysaccharides (Li et al., 2016). We have applied a modified controllable Fenton-system to obtain fCS oligosaccharides from *Isostichopus badionotus* with minimal impact on the main repeating structure and have named this oligosaccharide fraction DfCS-*Ib* (Li et al., 2017). The anticoagulant activity of DfCS-*Ib* has reduced side effects suggesting its potential therapeutic application (Li et al., 2017). However, the effects of DfCS-*Ib* on lipid metabolism remain undefined.

In the present study, DfCS-*Ib* prepared by our formerly reported method (Li et al., 2016), was explored for lipid regulation. The hypolipidemic activity of DfCS-*Ib* was investigated from lipid profile, inflammatory cytokines, and liver and epididymal fat histology. Related mRNA expression of adipose tissues and transcriptome analysis of liver were used here to reveal the possible mechanisms of DfCS-*Ib* effects on lipid metabolism disorders.

2. Materials and methods

2.1. Materials

Sea cucumbers *Isostichopus badionotus* (from Western Atlantic Ocean) were purchased from a local market in Qingdao, Shandong, China.

2.2. Preparation of sea cucumber oligosaccharides

Crude chondroitin sulfate from *Isostichopus badionotus* (fCS-*Ib*) was prepared and purified based on a previously described method (Chen et al., 2012). DfCS-*Ib* from *Isostichopus badionotus* was prepared by a newly developed method of oxidative degradation based on a previous report (Li et al., 2016). Reaction conditions were pH 6, 200 mM H_2O_2, 2 mM Cu^{2+} and temperature at 65 °C. The fCS-*Ib* (1000 mg) starting material was dissolved in 250 mL 0.1 M sodium acetate-acetic acid solution containing copper (II) acetate and adjusted the valve to pH 6. Hydrogen peroxide was added with mixing and the reaction was maintained at 65 °C for 5 h. Chelex 100 resin was added to remove Cu^{2+} and terminate the reaction. The depolymerized products were desalted by dialysis with a 500 Da cut-off membrane for 72 h, concentrated and subsequently lyophilized. The degree of degradation was analyzed using high performance gel permeation chromatography (GPC). GPC was performed on a Waters Ultrahydrogel 250 column (3.9 × 300 mm) (Milford, MA, USA) eluted with 0.2 M aqueous NaCl solution at a flow rate 0.5 mL/min and monitored using a refractive index detector. Glucan standards were used to determine the molecular weight of the samples. A final molecular weight of DfCS-*Ib* was determined to be 4.3 kDa (Supplementary Fig. 1) with 1.8 polydispersity. DfCS-*Ib* contained glucuronic acid (GlcA), galactosamine (GalNAc), fucose (Fuc) and sulfate at a molar ratio of 1.3:1.0:1.7:3.1 (Supplementary Fig. 2). According to ^{1}H NMR (Supplementary Fig. 3), DfCS-*Ib* was a fucosylated CSE with a 2, 4-*O*-sulfated fucose branch, which was consistent with former products (Li et al., 2016) and had a similar sulfation pattern with fCS-*Ib* (Chen et al., 2013).

2.3. Animals and experimental design

Forty C57BL/6 J mice, male, weighting from 24 ± 2 g, were purchased from the m Shanghai Slaccas Laboratory Animal Company (Certificate Number SCXK (hu) 2007-0005, Shanghai, China). The animals were housed in stainless steel cages at room temperature (25 ± 2 °C) and a 12 h light cycle, and fed with a commercial chow for a week to acclimatize to animal facilities. They were then weighed and randomly divided into five groups (8 mice each): Normal control was fed with regular chow, negative control group receive HFD (49.5% common chow + 15% sucrose + 20.4% lard + 12.3% protein + 2% premix compound + 0.8% maltodextrin) while the positive group receiving HFD and also a dose of 40 mg/kg/day simvastatin by intragastric gavage; Two groups receiving HFD were given DfCS-*Ib* in doses of 20, 40 mg/kg/day by intragastric gavage, which were referred to as DfCS-*Ib*-L and DfCS-*Ib*-H. The mice were allowed free access to food and water during the experimental period. Food consumption and weight gain were measured once each week. All animal maintenance and use procedures were in accordance with the guidelines of the Laboratory Animal Centre at Zhejiang University.

2.4. Biochemical analysis of serum

After 6 weeks, the mice were withheld food for at least 12 h, weighed and blood samples were collected from the retro-orbital puncture. Then, liver, kidney and white adipose tissue were collected, weighted, and frozen at −80 °C. Serum TC, TG, HDL-C, and LDL-C levels were measured enzymatically by commercial kit. Serum TNF-α and IL-6 contents were measured using commercial ELISA kits (R&D Systems, USA).

2.5. Liver and epididymal fat histology

After the blood samples were gathered, the liver and epididymal fat tissue samples were collected. Tissues were fixed with neutral formalin solution for 48 h, dehydrated through ascending grades of alcohol, cleared in benzene and embedded in low melting point paraffin wax. Sections, 3 μm thick, were cut and stained with hematoxylin and eosin (HE staining) for light microscopic examinations.

2.6. RT-qPCR analysis of subcutaneous adipose tissue

Total RNA in the adipose tissue was isolated using a total tissue TRIzol® Plus RNA Purification Kit (Invitrogen, America). Equal amounts of total RNA were used to synthesize cDNA with the Quant II fast RT kit (Tools, Taiwan). Quantitative real-time reverse-transcription PCR (RT–qPCR) was performed in triplicate using SYBR Green, 384-well plates and the CFX384 Touch Real-Time PCR System (Bio-Rad, USA). Each well was loaded with a total of 20 μL containing 1 μL of cDNA, 1 μL of target primers, and 8 μl of SDW and 10 μL of Power SYBR® Green Master Mix. Hot-start PCR was performed for 40 cycles, with each cycle consisting of denaturation for 15 s at 94 °C, annealing for 30 s at 60 °C and elongation for 30 s at 72 °C A housekeeping gene 18 sRNA was used as a control. PCR products were quantitated using the software iCycler iQ5 (Bio-Rad, USA). The mRNA relative expression levels were expressed as the ratio of signal intensity for the target genes to that of 18 sRNA. The primers of related genes were shown in the Supplementary Table 1

2.7. RNA-seq and bioinformatics

Total RNA was isolated from liver using the Trizol (Invitrogen) according to the manufacturer's protocol. RNA purity was assessed using the ND-1000 Nanodrop. Each RNA sample had an A260:A280 ratio above 1.8 and A260:A230 ratio above 2.0. RNA integrity was evaluated using the Agilent 2200 TapeStation (Agilent Technologies, USA) and

each sample had the RINe above 7.0. Briefly, rRNAs was removed from Total RNA using Epicentre Ribo-Zero rRNA Removal Kit (Illumina, USA) and fragmented to approximately 200bp. Subsequently, the purified RNAs was subjected to first strand and second strand cDNA synthesis following by adaptor ligation and enrichment with a low-cycle according to instructions of NEBNext® Ultra™ RNA Library Prep Kit for Illumina (NEB, USA). The purified library products were evaluated using the Agilent 2200 TapeStation and Qubit®2.0(Life Technologies, USA) and then diluted to 10 pM for cluster generation in situ on the HiSeq2500 pair-end flow cell followed by sequencing (1 × 50 bp) on HiSeq 2500. Reads were aligned to the mouse transcriptome (mm10, Ensembl v73). Reads were aligned using bowtie (v1.0.1) and RSEM (v1.2.12) (Li & Dewey, 2011). The raw transcriptome data were deposited in the Gene Expression Omnibus (GEO; accession number, GSE110526; https://www.ncbi.nlm.nih.gov/geo/query/acc.cgi?acc=GSE110526).

A $|\log2FoldChange| > 1$ and Q-value < 0.001 were used to determine significance. Gene Ontology (GO) enrichment analysis of differentially expressed transcripts was implemented by the GOSeq R package, in which gene length bias was corrected. Kyoto Encyclopedia of Genes and Genomes (KEGG) biochemical pathways analysis was also performed by the web tool KEGG.

2.8. Statistical analysis

All of the numeric results are the mean ± SD. Repeated measures ANOVA was used to evaluate any changes in food utilization among groups. Other comparisons among the groups were performed with one-way ANOVA followed by a LSD (Least Significant Difference) or Duncan's test. SPSS 20 was used for all analysis. Differences were defined as statistically significant for values of $p < 0.05$.

3. Results and discussion

3.1. Effects of DfCS-Ib on body weight, liver weight, kidney weight, epididymal fat mass and food intake

The mice were fed with a HFD containing 45% fat for six weeks to build a hyperlipidemic model, which leading to significant gain in body, liver, kidney and epididymal fat weight compared with animals fed chow feeding (Fig. 1). Weight gain of the HFD group was 4.36 ± 0.92 g (Fig. 1a), twice of the control group (2.28 ± 0.63 g, $P < 0.05$ compared to HFD group). The body weight gains of simvastatin, DfCS-*Ib*-L (20 mg/kg), and DfCS-*Ib*-H (40 mg/kg) treated animals showed no significant difference with the control group ($P > 0.05$), but showed much lower values than the HFD group ($P < 0.05$). Consistent with the weight gains, animals receiving HFD had higher liver, kidney, and epididymal fat weight ($P < 0.05$ compared to control group), while simvastatin, DfCS-*Ib*-L, and DfCS-*Ib*-H showed lower liver, kidney weight, and epididymal fat weight compared with the HFD group ($P < 0.05$). However, food consumption measured once a week indicated simvastatin group had a lower food intake, while there were no significant differences between control group, HFD group, and two DfCS-*Ib* groups on food consumption. These results suggested that DfCS-*Ib* inhibited the obesity caused by HFD even at a low dosage, without affecting the food consumption.

3.2. Effects of DfCS-Ib on biochemical parameters

Lipid profile of the HFD group showed significant increases in serum TC, TG, and LDL-C levels and decreases in serum HDL-C level compared to the control group, which can be reversed in the simvastatin group ($P < 0.05$, Table 1). DfCS-*Ib* treatment has a similar effect as simvastatin in decreasing the LDL-C, TC and TG levels and increasing the level of HDL-C ($P < 0.05$, compared with HFD mice), and showed a dose–dependent effect (comparing by DfCS-*Ib*-L and DfCS-*Ib*-H).

Serum glucose and insulin were also measured in the Table 1. HFD significantly increased serum glucose level ($P < 0.05$, compared with the control group). Supplement with simvastatin and DfCS-*Ib* decreased serum glucose level in HFD-fed mice ($P < 0.05$, compared with the HFD group). However, there was no significant difference about serum insulin between five groups. A HFD containing 45% calories from fat for six weeks may be not effective to cause insulin resistance.

Significant increases of serum TNF-α and IL-6 levels were observed in HFD group compared to the normal control group (Table 1). Oral intake of DfCS-*Ib* could significantly decrease the TNF-α and IL-6 level (comparing to HFD group, $P > 0.05$), while the commercial drug simvastatin have no significant effect. TNF-α and IL-6 are important pro-inflammatory cytokines (Kiecoltglaser et al., 2003). The chronic inflammatory response would be caused by obesity and enhanced production of IL-6 and TNF-α (Park et al., 2010). Our results suggest apart from regulating the lipid disorder, DfCS-*Ib* can also alleviate the low-level inflammatory status caused by HFD, especially with regards to the TNF-α level ($P > 0.05$, compared with control group).

3.3. Effects of DfCS-Ib on liver and fat tissue histology

Liver plays a key role in lipid metabolism, which is the hub of fatty acid synthesis and lipid circulation (Tessari, Coracina, Cosma, & Tiengo, 2009). The changes in liver histology are presented in Fig. 2. The normal mice showed orderly arrangements of hepatic cell cords, abundant cytoplasm, round central nucleus and distinct cell borders (Fig. 2a), while the HFD group showed enlargement of liver cell volume, the structural disorder of hepatic lobules, and visible cavitation within the cytoplasm characterized by macrovesicular steatosis of hepatocytes (Fig. 2b). Compared with the HFD group, a relatively normal structure of hepatic lobules, significantly improved fatty degeneration of liver cells in hepatic lobules and less visible necrosis of hepatocytes were noted in groups with treatment (Fig. 2**c–e**). DfCS-*Ib* (DfCS-*Ib*-L, Fig. 2**d** and DfCS-*Ib*-H, Fig. 2e) had similar effect as on simvastatin reducing the accumulation of lipid droplets in the hepatocytes of hyperlipidemic mice and improving liver function.

Adipose tissue has been the main site of storage of excess energy derived from food intake in a highly concentrated form as TG. Excess caloric intake will lead to increased TG input and adipocyte enlargement (Guilherme, Virbasius, Puri, & Czech, 2008), thus inducing fat hypertrophy. Therefore, the adipocyte size of the epididymal adipose tissue of the mice was examined by H&E staining (Fig. 3). The white adipocytes of the HFD group were much smaller than those of control group (Fig. 3**a** and **b**). With the treatment of simvastatin, DfCS-*Ib*-L, and DfCS-*Ib*-H, the size of white adipocytes was reduced to normal level. This indicated that DfCS-*Ib* could also efficiently reduce the lipid accumulation of adipocytes.

According to our results, both the histology of the liver and fat tissue suggested that the DfCS-*Ib* could maintain their normal morphology. Both of these are important organs involving in lipid metabolism. Thus, in the following parts, we investigated the influences of DfCS-*Ib* on the fat tissue and liver of HFD-fed mice by qRT-PCR and transcriptome respectively.

3.4. Effects of DfCS-Ib on the gene expression of fat tissue in HFD-fed mice

Adipose tissue is a complex organ that regulates and coordinates energy homeostasis (Cristancho & Lazar, 2011). Adipose tissue is mainly comprised of adipocytes, while other cell types, such as preadipocytes, lymphocytes, and macrophages also contribute to the function of adipose tissue. When excessive energy influx, the ability of adipocytes to function as endocrine cells and secrete multiple biologically active proteins is affected. Meanwhile, adipose tissue would secrete pro-inflammatory cytokines under the stimulation of over nutrition, and these local cytokines recruit more macrophages infiltrating into adipose tissue (Weisberg et al., 2003), initiating the development

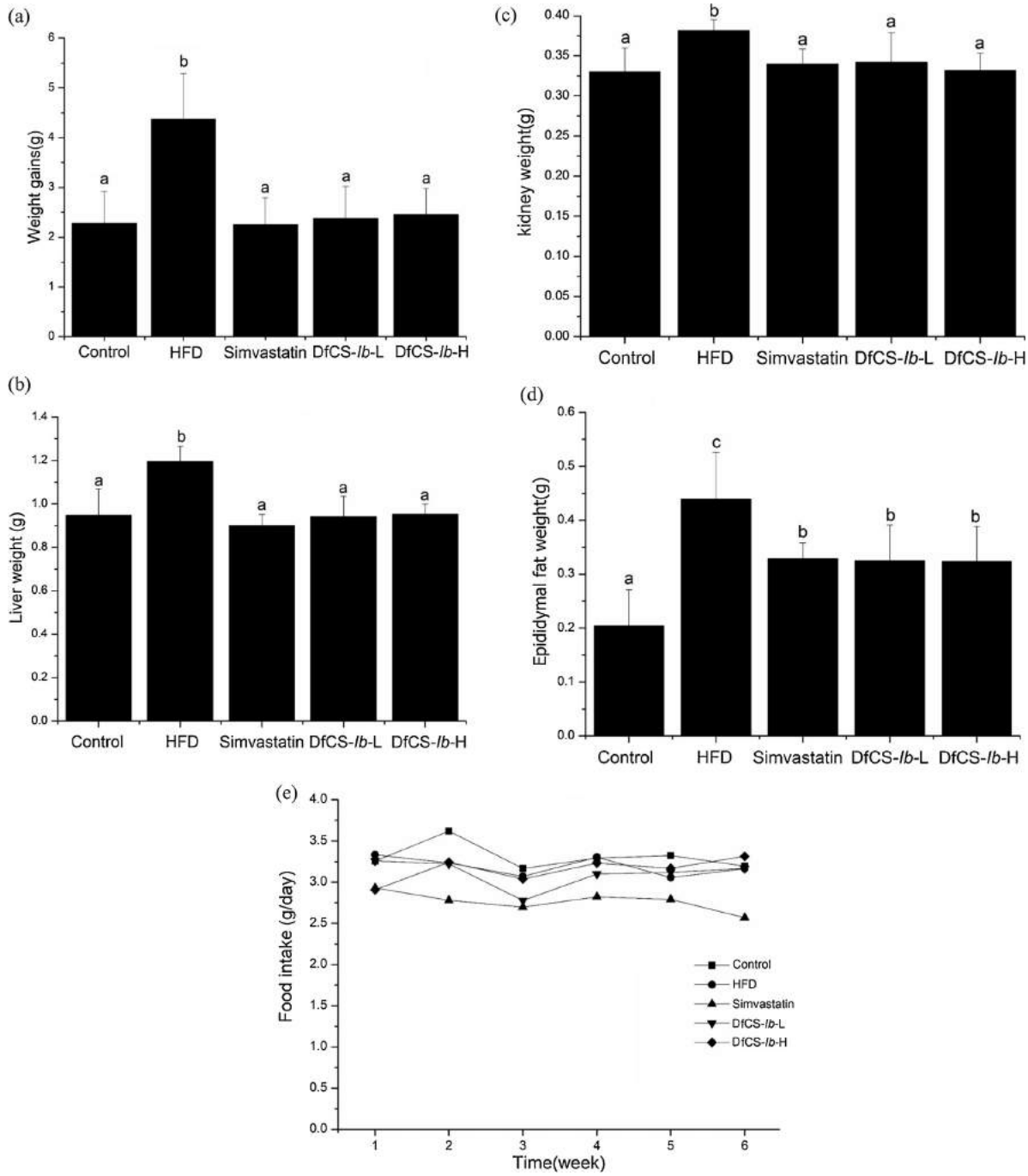

Fig. 1. (a) The final body weight gains of control group, HFD group, simvastatin, DfCS-*Ib*-L, DfCS-*Ib*-H group compared with initial weight at sixth week;(b) Effects of simvastatin, DfCS-*Ib*-L, DfCS-*Ib*-H on liver weight;(c) Effects of simvastatin, DfCS-*Ib*-L, DfCS-*Ib*-H on kidney weight;(d) Effects of simvastatin, DfCS-*Ib*-L, DfCS-*Ib*-H on epididymal fat weight. All data are expressed as mean ± SD (n = 8). (e) Food intake of control group, HFD group, Simvastatin, DfCS-*Ib*-L, DfCS-*Ib*-H.

of inflammation. Thus, the mRNA expression of some proteins in adipose tissues, were studied, including PPARγ, leptin, aP2, and F4/80. Since a high dosage, 40 mg/kg, had more profound affect in improving lipid profile, this dose was selected to investigate possible mechanisms.

The mRNA expression of peroxisome proliferators activated receptor γ (PPARγ) significantly decreased in the HFD group as compared to control ($P < 0.05$, shown in the Fig. 4a). Administration of either DfCS-*Ib* or simvastatin significantly attenuated this decrease compared to the untreated HFD group ($P < 0.05$). Meanwhile, the effects of DfCS-*Ib* on improving PPARγ level were better than that of simvastatin. PPARγ is responsible for adipocyte differentiation and fat storage that prevents lipotoxicity and allows for optimum insulin signaling (Zheng et al., 2011). Meanwhile, PPARγ also mediates HFD-induced hypertrophy of adipocytes and the activation of it can decrease diet-induced obesity (Lodhi et al., 2012). Our results suggested that HFD disturbed the expression of PPARγ in adipose tissue, while treatment with DfCS-*Ib*

Table 1
Effects of simvastatin, DfCS-*Ib*-L, and DfCS-*Ib*-H on the serum biochemical parameters of HFD-fed mice.

Groups	Control	HFD	Simvastatin	DfCS-*Ib*-L	DfCS-*Ib*-H
TC(mmol/L)	2.74 ± 0.39*	4.64 ± 0.79#	2.46 ± 0.15*	2.42 ± 0.18*,#	2.14 ± 0.18*,#
LDL-C(mmol/L)	1.66 ± 0.47*	2.31 ± 0.37#	1.73 ± 0.17*	1.97 ± 0.32#	1.64 ± 0.22*
HDL-C(mmol/L)	2.52 ± 0.53*	2.06 ± 0.37#	2.56 ± 0.27*	2.11 ± 0.33	2.35 ± 0.38
TG(mmol/L)	1.29 ± 0.18*	1.83 ± 0.47#	1.08 ± 0.04*	1.42 ± 0.14*	1.30 ± 0.07*
Glucose(mmol/L)	3.77 ± 0.60*	6.71 ± 0.36#	5.80 ± 1.01*,#	4.76 ± 0.88*,#	4.67 ± 0.86*,#
Insulin(mIU/L)	61.20 ± 9.87	74.17 ± 7.01	61.45 ± 11.34	69.76 ± 11.41	66.74 ± 10.53
TNF-α(ng/L)	25.98 ± 1.16*	29.29 ± 2.34#	28.62 ± 2.81#	25.37 ± 1.51*	26.19 ± 1.11*
IL-6(ng/L)	18.25 ± 1.52*	21.56 ± 0.85#	21.63 ± 0.91#	21.44 ± 2.41#	20.56 ± 1.30#

* $P < 0.05$: compared with HFD group.
# $P < 0.05$: compared to normal control group. Data are presented as mean ± SD, n = 8.

improved it to the normal level as the control group.

The mRNA expressions of leptin significantly increased in the HFD group as compared to the control ($P < 0.05$, shown in the Fig. 4b). Both DfCS-*Ib* and simvastatin reversed these abnormal expressions caused by HFD. Although the mRNA expressions of leptin in DfCS-*Ib* and simvastatin groups were higher than control groups ($P < 0.05$), they still significantly lowered leptin expression increased by HFD ($P < 0.05$). The adipokine leptin is a hormone specially secreted by adipocytes, and circulating leptin serves to communicate the state of body energy repletion to the central nervous system in order to control appetite (Myers, Cowley, & Munzberg, 2008). However, obese individuals often show high leptin level (leptin resistance) and leptin level has a positive correlation with glucose and TG levels (Ahima, 2008).

As shown in the Fig. 4**(c)**, HFD increased expression of adipocyte fatty-acid-binding protein (aP2) compared with the control group ($P < 0.05$). The simvastatin group showed significantly lower aP2 mRNA expression, which was even lower than the control group. DfCS-*Ib* groups can also decrease the expression of aP2 in HFD-fed mice. AP2 is expressed in adipocytes and macrophages, and integrates inflammatory and metabolic responses. Targeting aP2 with inhibitors can be a powerful therapy to prevent and treat metabolic diseases such as type 2 diabetes and atherosclerosis (Furuhashi et al., 2007).

In addition, the mRNA expression of macrophage-specific maker (F4/80) in HFD group was increased (Fig. 4d, $P < 0.05$ compared with the control group). Administration of either DfCS-*Ib* or simvastatin could restore the F4/80 expression to normal levels ($P > 0.05$ compared with control group). F4/80 is a maker for macrophages (Huang et al., 2016). Reducing in F4/80 expression suggesting that DfCS-*Ib* can efficiently reduce the macrophages infiltrating into adipose tissue. All our results indicated that DfCS-*Ib* could restore the function of adipose tissues and alleviate the inflammation caused by HFD.

3.5. Effects of DfCS-Ib on the lipid metabolism of liver by transcriptome analysis

The liver plays a key role in lipid metabolism, including lipogenesis, lipolysis, and transportation (Nguyen et al., 2008). These metabolic process are involved in a number of pathways. Transcriptome analysis was a powerful tool that can provide a large amount of metabolic information. This method can be used to help predict the roles of individual genes activated in response to external stimuli (Wang et al., 2017b). Thus, transcriptome analysis was used here to explore the damages of HFD on liver lipid metabolism and protective effects of DfCS-*Ib*. Volcano Plots of the observed changes in hepatic genes are shown in the Fig. 5. Compared with the control group, there were 640 up-regulated genes and 269 down-regulated genes in the HFD group (Fig. 5a). For the DfCS-*Ib* group, only 219 genes were up-regulated and 57 genes were down-regulated compared with the control group (Fig. 5b). These results suggest that HFD could change the expression of some genes and disturb normal metabolisms. However, there were fewer changes for genes in DfCS-*Ib* group. According to the KEGG Pathway Database and GO analysis, genes involving in lipid biosynthesis, degradation, and transportation were changed by HFD. These differentially expressed genes are summarized in Table 2.

The gene expression levels of Fasn, Acsl3, Acsl5, Elovl3, Elovl6,

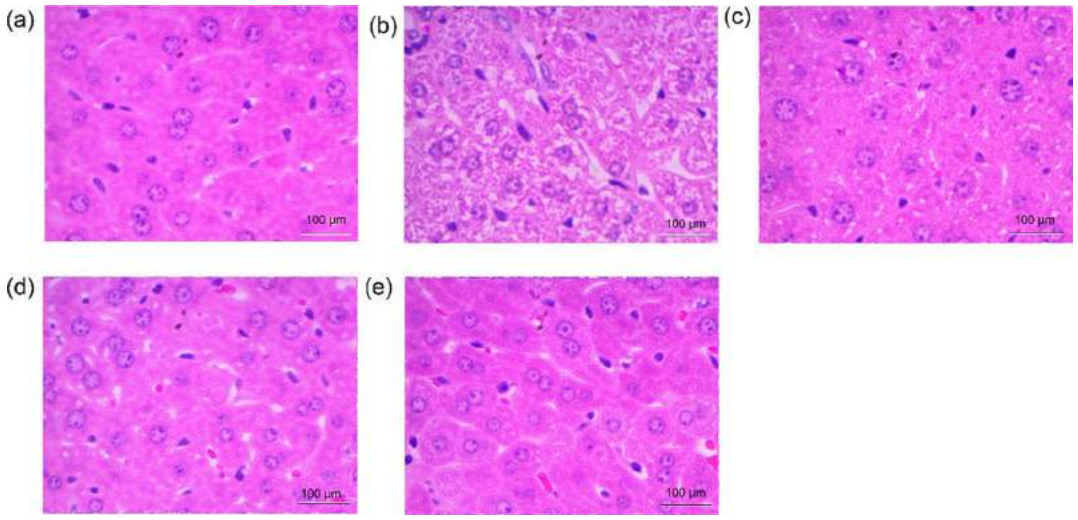

Fig. 2. histological assessment of livers in high fat diet-induced obesity mice(H&E stain, 200 × magnification) (a) control, (b) HFD, (c) Simvastatin, (d) DfCS-*Ib*-L, (e) DfCS-*Ib*-H.

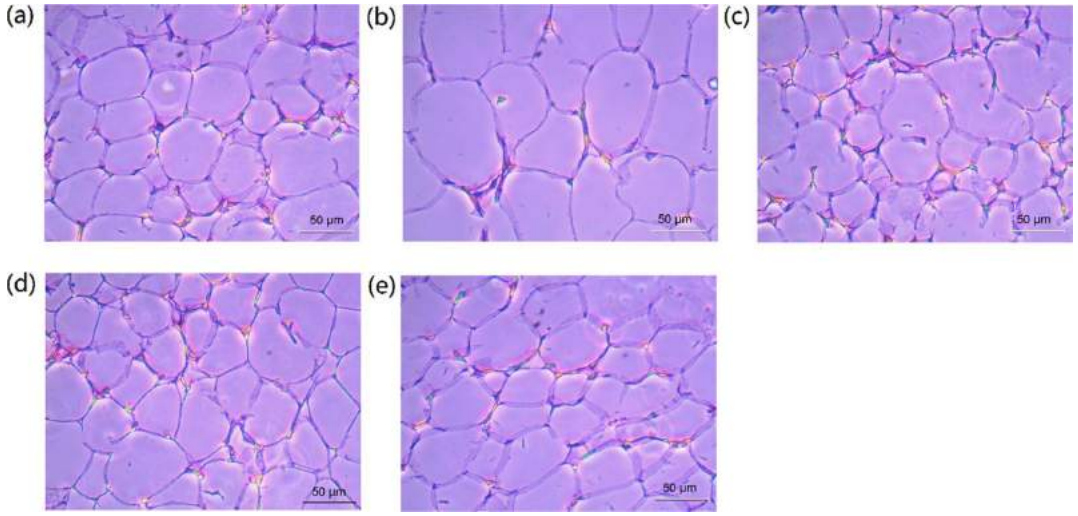

Fig. 3. histological assessment of epididymal adipose tissue in high fat diet-induced obesity mice(H&E stain, 400 × magnification) (a) control, (b) HFD, (c) Simvastatin, (d) DfCS-*Ib*-L, (e) DfCS-*Ib*-H.

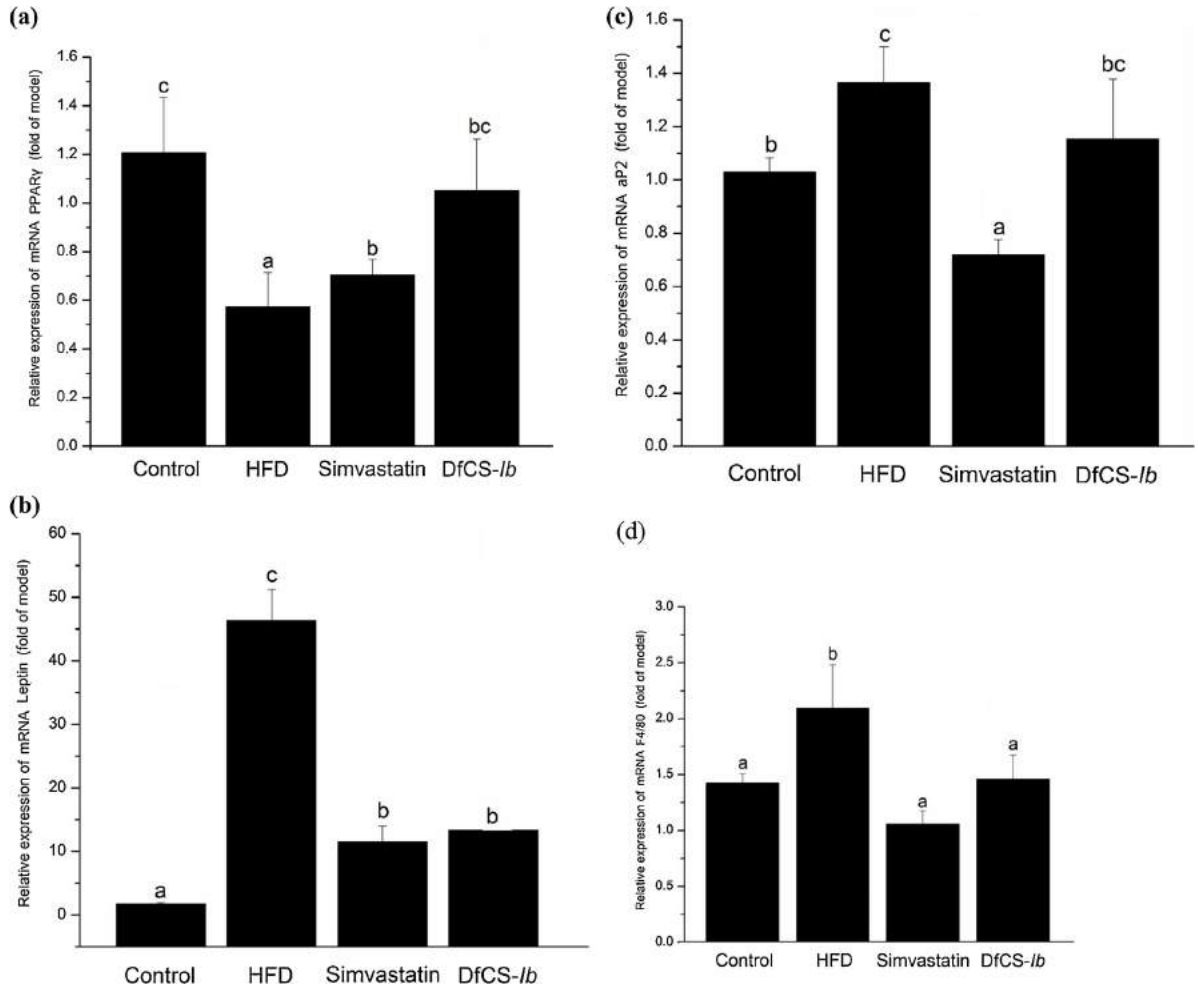

Fig. 4. Effects of DfCS-*Ib* on mRNA expression of PPARγ (a), leptin (b), aP2(c), and F4/80 (d) in the adipose tissues of mice fed on HFD using qRT-PCR. The results were normalized against 18 sRNA. Data are expressed as mean ± SD (n = 4). a, b, c: $P < 0.05$, compared between four groups.

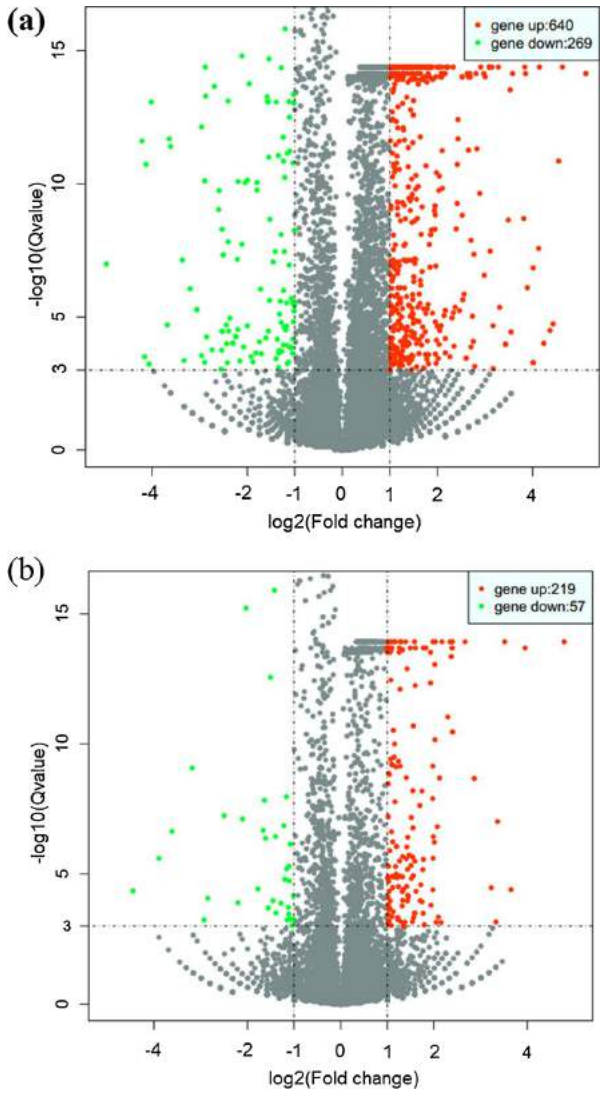

Fig. 5. (a) Volcano plot of control group compared with HFD group ; (b) Volcano plot of DfCS-*Ib* group compared with HFD group. A |log2FoldChange| > 1 and Q-value < 0.001 were used to determine significance. Genes that log2FoldChange > 1 and Q-value < 0.001 were represented by red spots, while genes that log2FoldChange < -1 and Q-value < 0.001 were represented by green genes (For interpretation of the references to colour in this figure legend, the reader is referred to the web version of this article).

Scd1 and Scd2, involving in lipogenesis (Matsuzaka et al., 2012), were increased by HFD. In contrast, the gene expression levels of ACOTs, CPT1α and Ehhadh involved in lipid β-oxidation were significantly decreased in the HFD group. Genes related to steroid biosynthesis such as Fdft1, Sqle, Lss, Msmol, Nsdhl, Sc5d, Dhcr7, Soat2 were up-regulated by HFD. In addition, some genes of 17β-HSD family (Hsd17β2 and Hsd17β12) and 3β-HSD family (Hsd3β2, Hsd3β3, Hsd3β5, and Hsd3β7) were up-regulated by HFD. 17beta-Hydroxysteroid dehydrogenases (17beta-HSDs) are important enzymes in steroid metabolism (He et al., 2017; Moeller & Adamski, 2009). 3beta-Hydroxysteroid dehydrogenases (3beta-HSDs) are involved in the biosynthesis of nearly all steroid hormones, inhibition of 3β-HSD could represent a potential target for the treatment of hormone dependent cancers (Klisuric et al., 2016). Cytochrome P450 (P450) enzymes are important in the metabolism of drugs, steroids, fat-soluble vitamins, carcinogens, pesticides, and many other types of chemicals. Their catalytic activities are important issues in areas such as drug–drug interactions and endocrine function (Guengerich, Waterman, & Egli, 2016). In our study, Cyp7a1 was down-regulated and Cyp4a12a, CYP51, and Cyp2r1 were up-regulated by HFD. The expression of PPARγ was increased in HFD group. Unlike the expression in adipose tissue, PPARγ in liver was up-regulated by HFD. It has been reported that PPARγ is expressed at elevated levels in the liver of murine models of diabetes or obesity caused by HFD intervene (Matsusue et al., 2003). These results indicated that HFD disrupted the balance of lipid metabolism in liver. When intervened with DfCS-*Ib* group, the levels of these genes mentioned above were restored in different degrees, similar to the expressions observed for the control group (Table 2). DfCS-*Ib* could reverse the imbalance and keep the lipid metabolism by reducing genes expression involving in lipid lipogenesis and increasing lipidolysis.

QRT-PCR analysis was performed to confirm the changes in expression of some of these genes by using the same mice liver samples used in the above transcriptome sequencing (as shown in the Fig. 6). The results of qRT-PCR showed that the gene expression profiles were very similar to the transcriptome sequencing results.

4. Further discussion for possible mechanism of DfCS-*Ib* on lipid disorders

In the present work, even low-doses of DfCS-*Ib* could alleviate damage with the same power simvastatin. DfCS-*Ib* can restore lipid profile, alleviate mild inflammation, inhibit adipocyte hypertrophy, and maintain normal histomorphology of liver caused by HFD. Former studies reported that sulfated polysaccharides such as carrageenan and its low molecular weight carrageenan derivatives can be proinflammatory agent (Tobacman, Bhattacharyya, Borthakur, & Dudeja, 2008). Our results showed that DfCS-*Ib* inhibited inflammation by reducing serum TNF-α and IL-6. Meanwhile, DfCS-*Ib* alleviated inflammation in the fat tissue by reducing macrophages. There are a limited number of studies on the effect of oligosaccharides on lipid metabolism disorder and none provide a possible mechanism. Pectic oligosaccharides significantly lowered the serum levels of TC and TG in hyperlipidemia mice induced by HFD (Li et al., 2010). Chitosan oligosaccharide reduce lipid accumulation in liver, improve multiple both in liver and serum, and normalize mRNA expression of liver peroxisome proliferator-activated receptor-α (PPARα) and hepatic lipase (HL) (Pan et al., 2016).

Here, we used transcriptome to explore the possible mechanism of DfCS-*Ib* on lipid disorders caused by HFD. Treatment with DfCS-*Ib* could down-regulate genes involving in the lipid synthesis and up-regulate genes involving in lipid oxidation. This indicated DfCS-*Ib* inhibits lipid disorders by promoting normal lipid metabolism in the liver. DfCS-*Ib* reduces lipid synthesis and promotes lipid lipidolysis, thus processing excessive lipid from HFD and reducing serum lipid. More importantly, some of these genes are involved in metabolic diseases caused by HFD. These metabolic diseases are often complications accompanied by lipid disorders. For example, Acsl5 ablation in mice could reduce adiposity, improve insulin sensitivity, increase energy expenditure, and delay triglyceride absorption (Bowman et al., 2016). Elovl6 is a critical modulator for atherogenic HFD–induced inflammation, oxidative stress, and fibrosis in the liver. High Elovl6 expression is positively correlated with severity of hepatosteatosis and liver injury in NASH patients (Matsuzaka et al., 2012). DfCS-*Ib* reduced the gene expression of Acsl5 and Elovl6 in the liver. Since liver lipid metabolism is a network involving many kinds of genes, it is too complex to distinguish a detailed mechanism. We hypothesize that of DfCS-*Ib* regulate one or several critical genes expression and then indirectly affect the network of genes expression in the liver. However, the exact mechanism of DfCS-*Ib* at on lipid metabolism needs additional experiments.

Table 2
Comparison of gene transcript patterns of lipid metabolism between control and HFD-fed mice with or without DfCS-*Ib* treatment.

Symbol	Gene ID	Gene name	log2 ratio	
			HFD	DfCS-*Ib*
Fasn	14104	fatty acid synthase	3.087	0.102
Acsl3	74205	acyl-CoA synthetase long-chain family member 3	1.768	−0.018
Acsl5	433256	acyl-CoA synthetase long-chain family member 5	1.179	0.379
Elovl3	12686	elongation of very long chain fatty acids (FEN1/Elo2, SUR4/Elo3, yeast)-like 3	1.257	0.805
Elovl6	170439	ELOVL family member 6, elongation of long chain fatty acids (yeast)	1.513	0.171
Scd1	20249	stearoyl-Coenzyme A desaturase 1	2.520	−0.742
Scd2	20250	stearoyl-Coenzyme A desaturase 2	1.224	0.493
Acot1	26897	acyl-CoA thioesterase 1	−2.069	−0.231
Acot2	171210	acyl-CoA thioesterase 2	−1.354	−0.461
Acot3	171281	acyl-CoA thioesterase 3	−2.068	−1.865
Acot4	171282	acyl-CoA thioesterase 4	−1.041	−0.603
CPT1α	12894	carnitine palmitoyltransferase 1a, liver	−1.283	−0.051
Ehhadh	74147	dehydrogenase	−1.502	−0.441
Fdft1	14137	farnesyl diphosphate farnesyl transferase 1	2.551	0.120
sqle	20775	squalene epoxidase	3.974	0.815
Lss	16987	lanosterol synthase	1.925	−0.089
Msmol	66234	methylsterol monoxygenase 1	3.834	1.176
Nsdhl	18194	NAD(P) dependent steroid dehydrogenase-like	3.708	0.476
Sc5d	235293	sterol-C5-desaturase	2.139	0.402
Dhcr7	13360	7-dehydrocholesterol reductase	1.969	−0.107
Soat2	223920	sterol O-acyltransferase 2	1.026	0.335
Cyp4a12a	277753	cytochrome P450, family 4, subfamily a, polypeptide 12α	1.111	0.273
Cyp7a1	13122	cytochrome P450, family 7, subfamily a, polypeptide 1	−1.385	−0.480
CYP51	13121	cytochrome P450, family 51	2.888	0.455
Cyp2r1	244209	cytochrome P450, family 2, subfamily r, polypeptide 1	1.115	0.255
Hsd17β12	56348	hydroxysteroid (17-beta) dehydrogenase 12	1.033	0.357
Hsd17β2	15486	hydroxysteroid (17-beta) dehydrogenase 2	1.042	0.518
Hsd3β2	15493	hydroxy-delta-5-steroid dehydrogenase, 3 beta- and steroid delta-isomerase 2	2.295	0.558
Hsd3β3	15494	hydroxy-delta-5-steroid dehydrogenase, 3 beta- and steroid delta-isomerase 3	2.524	1.237
Hsd3β5	15496	hydroxy-delta-5-steroid dehydrogenase, 3 beta- and steroid delta-isomerase 5	6.667	4.239
Hsd3β7	101502	hydroxy-delta-5-steroid dehydrogenase, 3 beta- and steroid delta-isomerase 7	1.431	0.501
Pparγ	19016	peroxisome proliferator activated receptor gamma	1.430	0.171

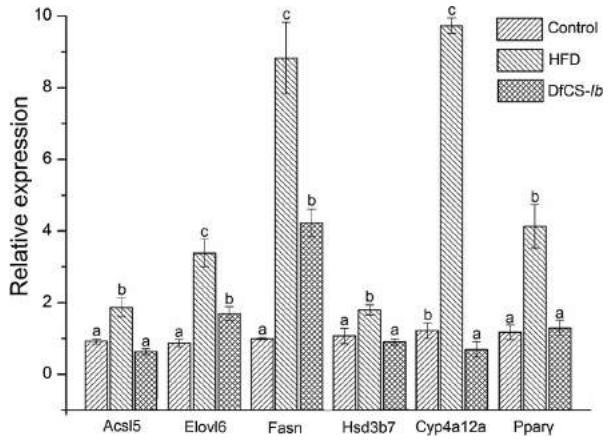

Fig. 6. Verification of Acsl5, Elovl6, Fasn, Hsd3b7, Cyp4a12a and Pparγ expression in the liver using qRT-PCR. The relative expression level of each sample was calibrated by the comparative threshold cycle method, using 18 s rRNA as an endogenous control. The analyses were performed in triplicate (n = 4). a, b, c < 0.05 compared between three groups.

5. Conclusions

Although fucosylated chondroitin sulfate oligosaccharides have been investigated extensively for its anticoagulation activity (Zhao et al., 2015), their effects on the dyslipidemia caused by HFD has not yet been defined. Our study supports the argument that HFD can result in many metabolic diseases such as lipid disorders, obesity, chronic inflammation and non-alcoholic fatty liver disease (NAFLD). DfCS-*Ib* supplementation significantly suppresses high-fat diet induced lipids disorders such as obesity, hyperlipidemia, and low-grade inflammation. Meanwhile, DfCS-*Ib* can balance the lipid trafficking by normalizing genes expression involving in lipid metabolism in adipose tissues and liver. Our study expands current understanding of hyperlipidemia induced by HFD and provides a potential interventional strategy by supplementing DfCS-*Ib*. These results suggest DfCS-*Ib* could not only be a kind of anticoagulant agent similar to more expensive commercial drugs such as heparin but also be a functional food regulating lipid disorders.

Appendix A. Supplementary data

Supplementary material related to this article can be found, in the online version, at doi:https://doi.org/10.1016/j.carbpol.2018.08.020.

References

Ahima, R. S. (2008). Revisiting leptin's role in obesity and weight loss. *Journal of Clinical Investigation, 118*(7), 2380–2383.
Ahn, M. Y., Hwang, J. S., Kim, M. J., & Park, K. K. (2016). Antilipidemic effects and gene expression profiling of the glycosaminoglycans from cricket in rats on a high fat diet. *Archives of Pharmacal Research, 39*(7), 926–936.
Bowman, T. A., O'Keeffe, K. R., D'Aquila, T., Yan, Q. W., Griffin, J. D., Killion, E. A., et al. (2016). Acyl CoA synthetase 5 (ACSL5) ablation in mice increases energy expenditure and insulin sensitivity and delays fat absorption. *Molecular Metabolism, 5*(3), 210–220.
Cao, Y., Zou, S., Xu, H., Li, M., Tong, Z., Xu, M., et al. (2016). Hypoglycemic activity of the Baker's yeast β-glucan in obese/type 2 diabetic mice and the underlying mechanism. *Molecular Nutrition & Food Research, 60*(12).
Chen, S., Hu, Y., Ye, X., Li, G., Yu, G., Xue, C., et al. (2012). Sequence determination and anticoagulant and antithrombotic activities of a novel sulfated fucan isolated from the sea cucumber Isostichopus badionotus. *Biochim Biophys Acta, 1820*(7), 989–1000.
Chen, S., Xue, C., Yin, L. A., Tang, Q., Yu, G., & Chai, W. (2011). Comparison of structures and anticoagulant activities of fucosylated chondroitin sulfates from different sea cucumbers. *Carbohydrate Polymers, 83*(2), 688–696.
Chen, S. G., Li, G. Y., Wu, N. A., Guo, X., Liao, N. B., Ye, X. Q., et al. (2013). Sulfation

pattern of the fucose branch is important for the anticoagulant and antithrombotic activities of fucosylated chondroitin sulfates. *Biochimica Et Biophysica Acta-General Subjects, 1830*(4), 3054–3066.
Cordain, L., Eaton, S. B., Sebastian, A., Mann, N., Lindeberg, S., Watkins, B. A., et al. (2005). Origins and evolution of the Western diet: Health implications for the 21st century. *American Journal of Clinical Nutrition, 81*(2), 341–354.
Cristancho, A. G., & Lazar, M. A. (2011). Forming functional fat: A growing understanding of adipocyte differentiation. *Nature Reviews Molecular Cell Biology, 12*(11), 722–734.
Furuhashi, M., Tuncman, G., Gorgun, C. Z., Makowski, L., Atsumi, G., Vaillancourt, E., et al. (2007). Treatment of diabetes and atherosclerosis by inhibiting fatty-acid-binding protein aP2. *Nature, 447*(7147), 952–U959.
Guengerich, F. P., Waterman, M. R., & Egli, M. (2016). Recent structural insights into cytochrome P450 function. *Trends in Pharmacological Sciences, 37*(8), 625–640.
Guilherme, A., Virbasius, J. V., Puri, V., & Czech, M. P. (2008). Adipocyte dysfunctions linking obesity to insulin resistance and type 2 diabetes. *Nature Reviews Molecular Cell Biology, 9*(5), 367–377.
He, Z., Lv, F., Ding, Y. F., Huang, H. G., Liu, L., Zhu, C. Y., et al. (2017). High-fat diet and chronic stress aggravate adrenal function abnormality induced by prenatal caffeine exposure in male offspring rats. *Scientific Reports, 7*.
Hu, S., Chang, Y., Wang, J., Xue, C., Li, Z., & Wang, Y. (2013). Fucosylated chondroitin sulfate from sea cucumber in combination with rosiglitazone improved glucose metabolism in the liver of the insulin-resistant mice. *Bioscience Biotechnology & Biochemistry, 77*(11), 2263–2268.
Huang, X., Yu, T., Ma, C., Wang, Y., Xie, B., Xuan, D., et al. (2016). Macrophages play a key role in the obesity-induced periodontal innate immune dysfunction via nucleotide-binding oligomerization domain-like receptor protein 3 pathway. *Journal of Periodontology, 87*(6), 614.
Kakimoto, P. A., & Kowaltowski, A. J. (2016). Effects of high fat diets on rodent liver bioenergetics and oxidative imbalance. *Redox Biology, 8*, 216–225.
Kiecoltglaser, J. K., Preacher, K. J., Maccallum, R. C., Atkinson, C., Malarkey, W. B., & Glaser, R. (2003). Chronic stress and age-related increases in the proinflammatory cytokine IL-6. *Proceedings of the National Academy of Sciences of the United States of America, 100*(15), 9090–9095.
Klisuric, O. R., Szecsi, M., Djurendic, E. A., Nikoletta, S., Herman, B. E., Santa, S. S. J., et al. (2016). Structural analysis and biomedical potential of novel salicyloyloxy estrane derivatives synthesized by microwave irradiation. *Structural Chemistry, 27*(3), 947–960.
Kotani, K., Serban, M. C., Penson, P., Lippi, G., & Banach, M. (2016). Evidence-based assessment of lipoprotein(a) as a risk biomarker for cardiovascular diseases - some answers and still many questions. *Critical Reviews in Clinical Laboratory Sciences, 53*(6), 1.
Li, B., & Dewey, C. N. (2011). RSEM: Accurate transcript quantification from RNA-Seq data with or without a reference genome. *BMC Bioinformatics, 12*(1), 323.
Li, J., Shan, L., Yan, L., Tian, D., Linhardt, R. J., Yu, Y., et al. (2017). Fucosylated chondroitin sulfate oligosaccharides exert anticoagulant activity by targeting at intrinsic tenase complex with low FXII activation: Importance of sulfation pattern and molecular size. *European Journal of Medicinal Chemistry, 139*, 191.
Li, J. H., Li, S., Zhi, Z. J., Yan, L. F., Ye, X. Q., Ding, T., et al. (2016). Depolymerization of fucosylated chondroitin sulfate with a modified fenton-system and anticoagulant activity of the resulting fragments. *Marine Drugs, 14*(9), 170.
Li, T., Li, S., Du, L., Na, W., Mei, G., Zhang, J., et al. (2010). Effects of haw pectic oligosaccharide on lipid metabolism and oxidative stress in experimental hyperlipidemia mice induced by high-fat diet. *Food Chemistry, 121*(4), 1010–1013.
Lodhi, I. J., Yin, L., Jensen Urstad, Anne P. L., Funai, K., Coleman, T., Baird, John H., et al. (2012). Inhibiting adipose tissue lipogenesis reprograms thermogenesis and PPARγ activation to decrease diet-induced obesity. *Cell Metabolism, 16*(2), 189–201.
Matsusue, K., Haluzik, M., Lambert, G., Yim, S. H., Gavrilova, O., Ward, J. M., et al. (2003). Liver-specific disruption of PPAR gamma in leptin-deficient mice improves fatty liver but aggravates diabetic phenotypes. *Journal of Clinical Investigation, 111*(5), 737–747.
Matsuzaka, T., Atsumi, A., Matsumori, R., Nie, T., Shinozaki, H., Suzuki-Kemuriyama, N., et al. (2012). Elovl6 promotes nonalcoholic steatohepatitis. *Hepatology, 56*(6), 2199–2208.
Moeller, G., & Adamski, J. (2009). Integrated view on 17beta-hydroxysteroid dehydrogenases. *Molecular and Cellular Endocrinology, 301*(1-2), 7–19.
Myers, M. G., Cowley, M. A., & Munzberg, H. (2008). Mechanisms of leptin action and leptin resistance. *Annual Review of Physiology, 70*, 537–556.
Nguyen, P., Leray, V., Diez, M., Serisier, S., Bloc'H, J. L., Siliart, B., et al. (2008). Liver lipid metabolism. *Journal of Animal Physiology and Animal Nutrition, 92*(3), 272.
Noeman, S. A., Hamooda, H. E., & Baalash, A. A. (2011). Biochemical study of oxidative stress markers in the liver, kidney and heart of high fat diet induced obesity in rats. *Diabetology and Metabolic Syndrome, 3*(1), 1–8.
Ouchi, N., Parker, J. L., Lugus, J. J., & Walsh, K. (2011). Adipokines in inflammation and metabolic disease. *Nature Reviews Immunology, 11*(2), 85–97.
Pan, H., Yang, Q., Huang, G., Chen, D., Cao, P., Huang, L., et al. (2016). Hypolipidemic effects of chitosan and its derivatives in hyperlipidemic rats induced by a high-fat diet. *Food and Nutrition Research, 60*.
Park, E. J., Lee, J. H., Yu, G.-Y., He, G., Ali, S. R., Holzer, R. G., et al. (2010). Dietary and genetic obesity promote liver inflammation and tumorigenesis by enhancing IL-6 and TNF expression. *Cell, 140*(2), 197–208.
Tessari, P., Coracina, A., Cosma, A., & Tiengo, A. (2009). Hepatic lipid metabolism and non-alcoholic fatty liver disease. *Nutrition Metabolism and Cardiovascular Diseases, 19*(4), 291–302.
Tobacman, J. K., Bhattacharyya, S., Borthakur, A., & Dudeja, P. K. (2008). The carrageenan diet: Not recommended. *Science, 321*(5892), 1040–1041.
Wang, J. H., Hu, S. W., Jiang, W., Song, W. D., Cai, L., & Wang, J. F. (2016). Fucoidan from sea cucumber may improve hepatic inflammatory response and insulin resistance in mice. *International Immunopharmacology, 31*, 15–23.
Wang, K., Cao, P., Shui, W., Yang, Q., Tang, Z., & Zhang, Y. (2015). Angelica sinensis polysaccharide regulates glucose and lipid metabolism disorder in prediabetic and streptozotocin-induced diabetic mice through the elevation of glycogen levels and reduction of inflammatory factors. *Food & Function, 6*(3), 902.
Wang, B., Zhang, S., Wang, X., Yang, S., Jiang, Q., Xu, Y., et al. (2017a). Transcriptome analysis of the effects of chitosan on the hyperlipidemia and oxidative stress in high-fat diet fed mice. *International Journal of Biological Macromolecules, 102*, 104–110.
Wang, B., Zhang, S. C., Wang, X. Y., Yang, S., Jiang, Q. X., Xu, Y. S., et al. (2017b). Transcriptome analysis of the effects of chitosan on the hyperlipidemia and oxidative stress in high-fat diet fed mice. *International Journal of Biological Macromolecules, 102*, 104–110.
Weisberg, S. P., McCann, D., Desai, M., Rosenbaum, M., Leibel, R. L., & Ferrante, A. W. (2003). Obesity is associated with macrophage accumulation in adipose tissue. *Journal of Clinical Investigation, 112*(12), 1796–1808.
Wu, N., Zhang, Y., Ye, X., Hu, Y., Ding, T., & Chen, S. (2016). Sulfation pattern of fucose branches affects the anti-hyperlipidemic activities of fucosylated chondroitin sulfate. *Carbohydrate Polymers, 147*, 1.
Wydro, P., Krajewska, B., & HąC-Wydro, K. (2007). Chitosan as a lipid binder: A langmuir monolayer study of chitosan-lipid interactions. *Biomacromolecules, 8*(8), 2611–2617.
Zhang, J., Zhang, W., Mamadouba, B., & Xia, W. (2012). A comparative study on hypolipidemic activities of high and low molecular weight chitosan in rats. *International Journal of Biological Macromolecules, 51*(4), 504.
Zhao, L., Wu, M., Xiao, C., Yang, L., Zhou, L., Gao, N., et al. (2015). Discovery of an intrinsic tenase complex inhibitor: Pure nonasaccharide from fucosylated glycosaminoglycan. *Proceedings of the National Academy of Sciences of the United States of America, 112*(27), 8284.
Zheng, X. K., Zhang, L., Wang, W. W., Wu, Y. Y., Zhang, Q. B., & Feng, W. S. (2011). Anti-diabetic activity and potential mechanism of total flavonoids of Selaginella tamariscina (Beauv.) Spring in rats induced by high fat diet and low dose STZ. *Journal of Ethnopharmacology, 137*(1), 662–668.